ELSEVIER

Polymer 41 (2000) 3337–3347

polymer

A conformational model for poly(dichlorophosphazene) derived from molecular dynamics simulations

M.P. Tarazona*, E. Saiz

Departamento de Química Física, Universidad de Alcalá, 28871 Alcalá de Henares, Madrid, Spain

Received 15 June 1999; accepted 19 July 1999

Abstract

Molecular dynamics (MD) simulations have been performed for an oligomer of poly (dichlorophosphazene) (PDCPN) containing 56 repeating units i.e. $(PCl_2N)_{56}$, seeking for the orientations of the rotational angles over the P–N skeletal bonds. Two different molecular systems were simulated. In the first one, the chain was packed into a cubic lattice (i.e. a cubic box with periodic boundary conditions) having a side length of 22.1 Å in order to reproduce a density of about 1 g/cm^3, while in the second one, the chain was assumed to be alone in vacuo. In both systems, the allowed orientations for the skeletal bonds are *cis* ($\phi = 0$) and *trans* ($\phi = 180$) with a slight preference for this second orientation. However, a more detailed analysis shows that the lattice produces more extended conformations, and therefore larger molecular dimensions, than the isolated molecule. Thus, the chain in the lattice is formed by sequences of two or three bonds in the *trans* conformations separated by *trans–cis* (the average number of bonds in the all-*trans* conformation is $\langle n_t \rangle \approx 2.7$) with negligible incidence of *cis–cis* conformations. The *trans* sequences are shorter (i.e. $\langle n_t \rangle \approx 1.7$) in the isolated molecule and the presence of *cis–cis* orientations is noticeable. The a priori probabilities for all the allowed orientations of each pair of bonds obtained by MD simulations can be reproduced by a very simple RIS model that was employed for the evaluation of the unperturbed dimensions of long chains. The values obtained for the characteristic ratio were $C_\infty \approx 15.7$ in the case of the lattice and 8.0 for the isolated molecule, the former value being in better agreement with experimental results than the later one. Long range interactions, mainly due to van der Waals forces, may be responsible for the differences observed in the two systems simulated here, and could also explain the widely different experimental values of molecular dimensions reported for this kind of polymers. © 2000 Elsevier Science Ltd. All rights reserved.

Keywords: Conformational model for poly(dichlorophosphazene); Molecular dynamics simulations; Long-range interactions

1. Introduction

Polyphosphazenes (PPNs) are polymers formed by an inorganic backbone of P and N atoms with two side groups, that may be organic or inorganic, attached to each skeletal phosphorus atom. Thus, the simplest of all these polymers is the poly(dichlorophosphazene) (PDCPN) in which the two side groups are chlorine atoms, $(PCl_2N)_n$. All the other PPNs may be formally obtained by replacement of the chlorine atoms of PDCPN by other kind of groups and, indeed, this is exactly the way in which many of these polymers are synthesized.

Several hundreds of PPNs with very different side groups have been prepared up to date and their macroscopic properties have been studied seeking for practical applications, among which oil-resistant elastomeric materials, flame-resistant polymers and biomedical materials, especially the biocompatible polymers, can be cited as typical examples [1–3].

Despite the enormous interest that this kind of polymers arise in the technological field, molecular characterization of PPNs is still very rudimentary. For instance, glass transition temperatures T_g, have been measured for all the known PPNs, however there are few publications devoted to magnitudes such as unperturbed dimensions, dipole moments or viscosimetric parameters and, what is even worse, the reported values for these magnitudes are usually very different and, in many cases, contradictory [4,5].

But, if the experimental characterizations of PPNs are scarce, the number of theoretical calculations of molecular properties is even smaller. Some calculations on phosphazene compounds employing quantum mechanics [6–11], molecular mechanics [12–15] and molecular dynamics [16] procedures, have been reported. However, most of these calculations concern small molecules and it is rather difficult to generalize neither the procedures nor the

* Corresponding author. Tel.: +34-91-885-4664; fax: +34-91-885-4763.

0032-3861/00/$ - see front matter © 2000 Elsevier Science Ltd. All rights reserved.
PII: S0032-3861(00)00515-7

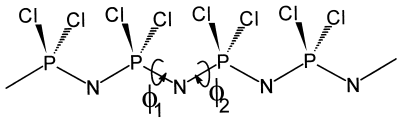

Fig. 1. Schematic representation of a segment of the poly(dichlorophosphazene) (PDCPN) chain in the all-*trans* conformation for which the rotational angles ϕ over the skeletal bonds NP–NP are taken to be 180°.

conclusions in order to apply them to polymers in solution. Several years ago, we developed a conformational model for PDCP based on molecular mechanics calculations [15] which gives a reasonable description of this polymer, and allows the evaluation of properties such as molecular dimensions with reasonable agreement between theoretical and experimental results. However, it is rather difficult to generalize this model in order to apply it to other PPNs with much more complicated side groups than simple chlorine atoms. Of course, it is quite simple to change the numerical values of the parameters in order to get an agreement with experimental results obtained by any PPN, but is more complicated to explain the reasons for those changes in basis of the molecular structures [17,18]. The reason of this difficulty lies in the molecular mechanics' scheme that gives serious problems when large side groups with many rotational angles should be taken into account and their conformational characteristics have to be merged with those of the main backbone. This difficulty may be surmounted with molecular dynamics procedures which allows the analysis of chains bearing almost any conceivable side groups. Following this idea, this study presents molecular dynamics simulations of an oligomer of PDCPN (the simplest of all PPNs, although we hope to be able to generalize for more complicated polymers) seeking for the conformational characteristics of the main chain that are then employed to set up an statistical model based on the rotational isomeric states scheme [19–21]. This model can be used to compute any conformational dependent property of the chain, and the evaluation of the unperturbed dimensions of the polymer is included as an example.

2. Molecular dynamics simulations

2.1. Molecular dynamics software

The DL_POLY package [22] was employed for all the MD simulations carried out in the preparation and warming up processes of the systems as well as in the data collection stages. A time step $\delta = 1$ fs (i.e. 10^{-15} s) was employed for the integration of the equations of motion. A multi-time step algorithm [23] with a secondary time step of 5 fs was employed in order to speed up the calculations. The temperature of the system was kept constant at $T = 300$ K while producing the data of interest by means of a Nose-Hoover thermostat [23] with a relaxation time of 500 fs. Cut-off distances $r_c = 9.6$ and 8 Å were employed, respectively for Coulombic and van der Waals interactions, i.e. interactions between atoms i and j were set to zero when their distance r_{ij} is larger than the appropriate r_c.

2.2. Molecular systems

All the MD simulations presented below were performed for an oligomer of poly(dichlorophosphazene) containing 56 repeating units PCl_2–N–. Fig. 1 shows a schematic representation of a segment of this chain in the all-*trans* conformation for which the rotational angles ϕ over the skeletal bonds NP–NP were taken to be 180°. Two different molecular systems, both based on the 56 units oligomer, were considered: for one of them, the chain was packed into a cubic lattice (i.e. a cubic box with periodic boundary conditions) having a side length $L = 22.1\,\AA$ in order to reproduce a density of about 1 g/cm^3, while in the second system, the chain was assumed to be alone in vacuo.

In the case of the lattice, the chain was first placed into a much larger box with $L_0 = 30\,\AA$ in order to avoid interpenetration among different segments which would produce unrealistically high values of energy, thus rendering difficult and unreliable any conceivable strategy for energy minimization. An MD simulation at high temperature (i.e. 1000 K) was then applied to this initial system, and the side of the box was decreased from the initial value L_0 to the final

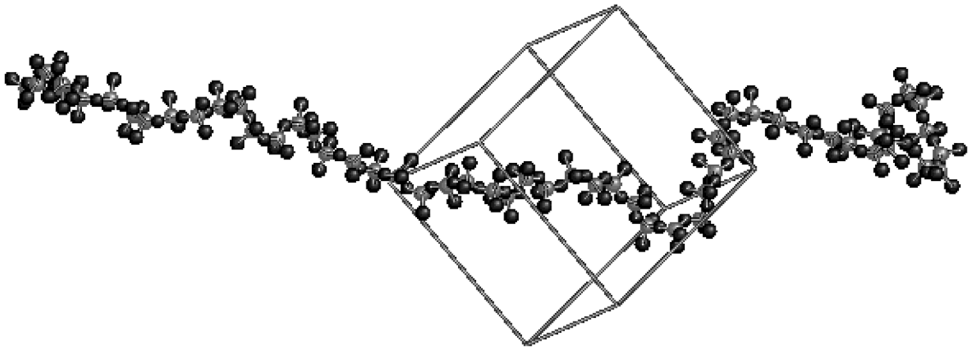

Fig. 2. One of the conformations adopted by the oligomer of PDCPN confined within a cubic lattice with periodic boundary conditions along the MD trajectory. Only a segment of the actual chain is in fact contained inside the cubic box which is filled up with images of several segments of the primary chain.

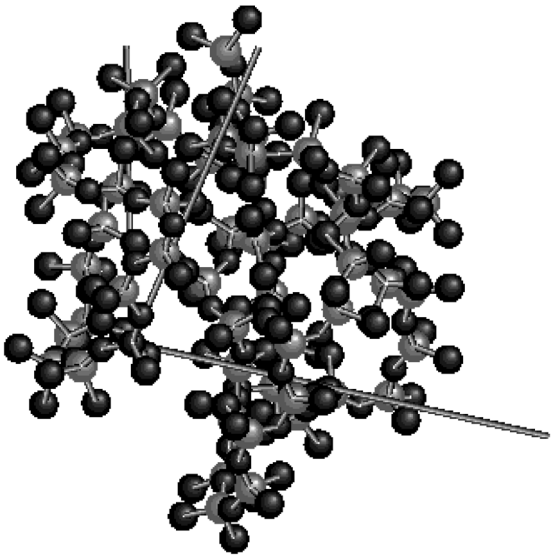

Fig. 3. One of the conformations adopted by the oligomer of PDCPN, treated as an isolated molecule, along the MD trajectory. An arbitrary coordinates system having axe lengths of 22.1 Å (the same than the side box on the lattice system), has been added in order to give an idea of the molecular dimensions.

Table 1
Set of parameters defining the force field employed for the present calculations (lengths in Å; angles in rad; energies in kcal/mol)

Bond stretching: $E_{bond} = \Sigma(k/2)(l - l_0)^2$			
Bond	k	l_0	Reference
Cl–P	403.2	1.99	[14]
N –P	849.6	1.57	[14]
Angle Bending: $E_{angle} = \Sigma(k/2)(\theta - \theta_0)^2$			
Angle	k	θ_0	Reference
P–N–P	36	131	[14]
N–P–N	129.6	121	[14]
N–P–Cl	86.4	108.4	[14]
Cl–P–Cl	216	102	[14]

Intrinsic Barriers: $E_{rot} = \Sigma(1/2)\{A_1[1 + \cos(\phi)] + A_2[1 - \cos(2\phi)] + A_3[1 + \cos(3\phi)]$				
Rotation	A_1	A_2	A_3	Reference
NP–NP	0.3 [14]	1.44	0	[14]
ClP–NP	0 [14]	0	0	[14]

vdW Interactions: $E_{vdw} = \Sigma 4\epsilon_{ij}[(\sigma_{ij}/r_{ij})^{12} - (\sigma_{ij}/\sigma_{ij})^6]$ with $\sigma_{ij} = (1/2)^{1/6}(r_i^0 + r_j^0)$; $\epsilon_{ij} = (\epsilon_I \epsilon_j)^{1/2}$			
Atom	ϵ_i	r_i^0	Reference
Cl	0.2245	1.975	[14][a]
P	0.2	2.1	AMBER [26–29]
N	0.16	1.75	AMBER [26–29]

[a] The equation employed in Ref. [14] for the vdW interactions is different from that of the AMBER force field. The values of ϵ_i and r_i^0 for the Cl atom were adjusted in order to obtain the same interactions with the equation of AMBER than those actually used in Ref. [14].

length L with increments of -0.5 Å and allowing a equilibration time of 1000 fs at each new size. Once the final volume was obtained, the system was cooled down to 50 K, with increments of -50 K and allowing equilibration times of 1000 fs at each new temperature, in order to minimize the energy and finally warmed up to the working temperature, again with increments of 50 K and thermostatization times of 1000 fs. All the simulations were thus performed under NVT conditions, i.e. canonical ensemble.

In the case of the isolated chain, the conformational energy was minimized with respect to all bond lengths, bond angles and rotations. The resulting optimized conformation was then warmed up by means of an MD simulation at increasing temperatures from 0 K to the working temperature with increments of 50 K, and allowing 1000 fs as equilibration time at each new temperature.

After all this preparation, the data collection process was started on each system. Thus, an MD simulation of 5×10^6 steps, covering a total time span of 5 ns, was carried out for each system, saving the magnitudes of interest for every $\Delta = 100$ fs, thus producing $N = 5 \times 10^4$ conformations of each system that were employed in posterior analysis. Figs. 2 and 3 represent one of the conformations adopted by the systems, lattice in Fig. 2 and isolated molecule in Fig. 3, along the MD trajectory. It is interesting to note that, as Fig. 2 shows, only a segment of the actual polymer chain lies in fact within the box defining the PBC, the rest of the box is occupied by images of the actual (or primary) chain. An arbitrary coordinates system having axes lengths of 22.1 Å (the same than the box side on the lattice system), has been added to the isolated molecule represented in Fig. 3 in order to give an idea of the molecular dimensions.

2.3. Force field

Many different force fields, designed for a wide variety of molecules, are available nowadays [24], but the applicability of most of these fields to PPNs is questionable, because atoms like P and Cl are not well parametrized. Calculations on PPN's have been performed employing very different force fields, from very simple ones that assumed fixed bond lengths and bond angles [12–15] to very sophisticated ones, like CHARMM [25] (Chemistry at HARvard Macromolecular Mechanics), including alternance of two different values for the main bond length on the polymer backbone [6,16]. Some attempts have also been made to derive a specific force field for PPNs from crystallographic data and employing either quantum [6,16] or molecular [14] mechanics calculations. However, it is difficult to ascertain at this moment which is the best force field for this kind of polymers, or even if the use of very sophisticated fields may be compensated by a better description of the system.

In fact, most of the calculations published up to date employing very different approaches agree in several significant features for this kind of polymers: The most stable orientations for the skeletal P–N bonds are *cis* ($\phi = 0$)

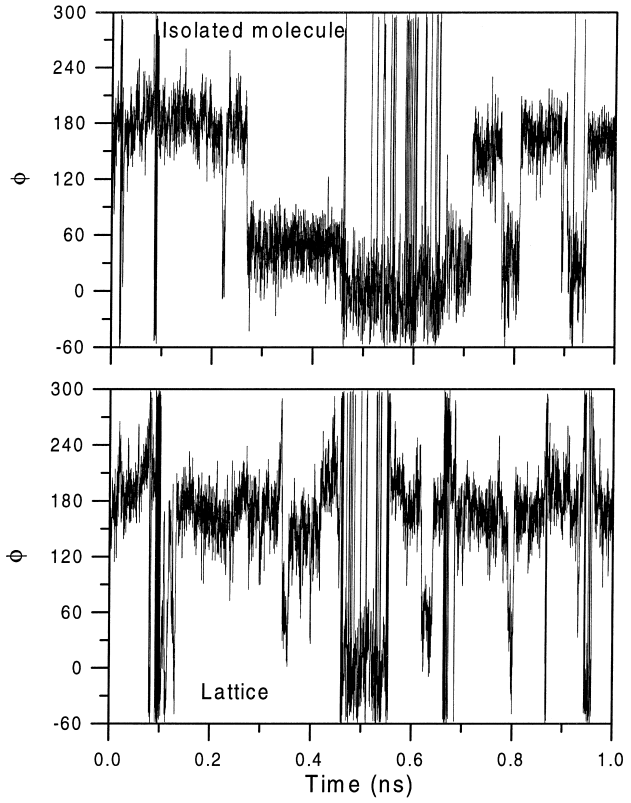

Fig. 4. The rotational angle over one of the skeletal bonds as function of time during the first nanosecond of the simulation. The rest of the simulation is not represented in order to enlarge the time axis.

and *trans* ($\phi = 180$) with a small preference for *trans*. The *gauche* states (i.e. local minima placed at $\phi \approx \pm 60°$) found in earlier calculations employing molecular mechanic procedures [15] vanish when the bond lengths and bond angles are allowed to fluctuate. However, the skeletal bonds may rotate without finding large energetic barriers, neither intrinsic nor produced by interatomic interactions, so that there is rather a fast interconversion from one to another state. Partial charges over P and N atoms of the backbone are quite large, and therefore, the Coulombic interactions are very strong. However, since there are both attractions and repulsions, these interactions play a rather minor role in the location of the conformational minima.

Most of the published papers dealing with molecular characteristics of phosphazenes are concerned with crystalline structures, or at least with solid samples, so that they pay much more attention to the location of the most stable structure than to the possible presence of other local minima and the passage from one to another, which is a key feature when studying the behavior of a polymer in solution.

For these reasons, we have chosen the AMBER [26–29] (Assisted Model Building with Energy Refinement) force field, which is very simple and quite popular, for the present work. The parameters that are not included in the standard set of AMBER were adjusted as to reproduce the same energies obtained by other authors [14]. Table 1 summarizes the set of parameters employed in our calculations. The total energy of a given conformation was evaluated as the sum of five contributions, namely: bond stretching, angle bending, intrinsic rotational barriers, van der Waals interactions and Coulombic energies. Thus,

$$E_{\text{total}} = E_{\text{bond}} + E_{\text{angles}} + E_{\text{rot}} + E_{\text{vdW}} + E_{\text{coul}} \quad (1)$$

Harmonic potentials were employed for both bond stretching and angle bending energies:

$$E_{\text{bond}} = \sum_{\text{bonds}} \frac{k}{2}(1 - 1_0)^2 \qquad E_{\text{angles}} = \sum_{\text{angles}} \frac{k}{2}(\theta - \theta_0)^2 \quad (2)$$

A triple cosine expression was employed for the intrinsic barrier over PN–PN rotational angles. However, no barrier was included for ClP–NP rotations. Thus,

$$E_{\text{rot}} = \sum_{\text{PN}-\text{PN}_{\text{rotat}}} \frac{1}{2}\{A_1[1 + \cos(\phi)] + A_2[1 - \cos(2\phi)] + A_3[1 + \cos(3\phi)]\} \quad (3)$$

The van der Waals interactions were represented by a Lennard-Jones potential among every pair of atoms separated by more than two bonds:

$$E_{\text{vdW}} = \sum_{i>j} 4\epsilon_{ij}\left[\left(\frac{\sigma_{ij}}{r_{ij}}\right)^{12} - \left(\frac{\sigma_{ij}}{r_{ij}}\right)^{6}\right] \quad (4)$$

with $\sigma_{ij} = (1/2)^{1/6}(r_i^0 + r_j^0)$ and $\epsilon_{ij} = (\epsilon_i \epsilon_j)^{1/2}$.

Interaction among partial charges assigned to every atom of the sample were employed for Coulombic interactions. Partial charges were computed for the cyclic trimer using the gaussian suite of programs [30]. The geometry was optimized at the restricted Hartree–Fock level of theory using the 6-311g** basis set, and a single point calculation on this geometry with a 6-311 + g(3df,2p) basis was performed for the calculation of the Mulliken charges. The values obtained, in units of electrons, were $q(\text{P}) = 1.821$; $q(\text{N}) = -0.919$ and $q(\text{Cl}) = -0.451$. A precision Ewald sum with a tolerance parameter of 10^{-6} was employed for the lattice, while in the case of the isolated molecule these interactions were computed by means of a Coulombic sum with distance dependent dielectrics, i.e. $\epsilon(r_{ij}) = \epsilon_0 r_{ij}$:

$$E_{\text{coul}} = 332.0 \sum_{i<j} \frac{q_i q_j}{\epsilon(r_{ij}) r_{ij}} = 332.0 \sum_{i<j} \frac{q_i q_j}{\epsilon_0 r_{ij}^2} \quad (5)$$

with a value $\epsilon_0 = 4$ for the effective dielectric constant of the medium in both systems.

A scaling factor of 1/2 was applied to both van der Waals and Coulombic 1–4 interactions, i.e. interactions among atoms separated by three bonds.

3. Results

The interest of the MD simulation was focused on a

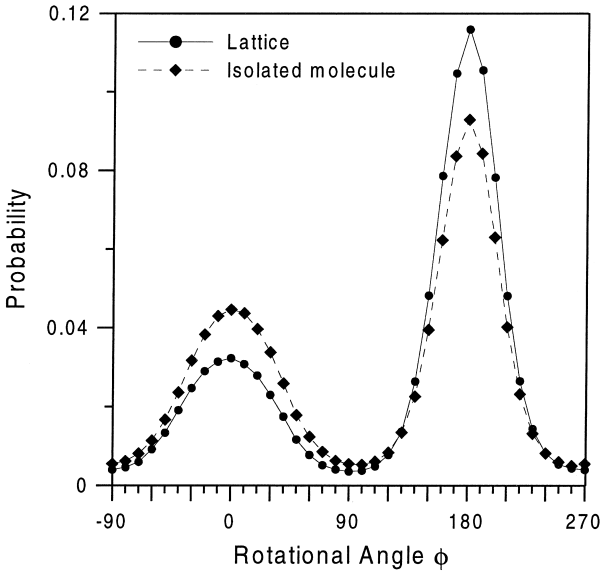

Fig. 5. Probability distributions for rotations over the skeletal bonds, assuming that each bond is independent of all its neighbors, averaged over the 18 bonds on the fragment of interest.

segment containing 18 skeletal bonds located at the center of the chain in order to avoid distortions produced by end effects so that the results obtained for this segment could be employed to represent skeletal bonds within a very long polymer chain. The value of the rotational angle ϕ over each of these 18 bonds was recorded every 100 integration steps so that the raw result of the simulation is a set of 5×10^4 values for each one of these 18 rotations. Fig. 4 shows the variation with time of one of these rotational angles, both for the lattice and for the isolated molecule, during the first nanosecond of the simulation. The results for the remaining 4 ns are very similar and are not shown in order to employ a larger scale for the time axis. As Fig. 4 indicates, the interconversion among *cis* ($\phi \approx 0$) and *trans* ($\phi \approx 180°$) states is rather fast so that the molecule visits all its allowed conformational space within the time of the simulation, and the results can be analyzed with statistical procedures.

The probability distribution of each rotatable bond on the fragment of interest, taken as independent of its neighbors, was computed by counting how many times along the simulation the studied angle reached a given value with a tolerance of $\pm 5°$, for instance, the results indicated for $\phi = 100$ represent the fraction of conformations in which $95 < \phi < 105$. The results, averaged over the 18 bonds under study, are depicted in Fig. 5, which clearly indicates that *cis* and *trans* are the two allowed rotational isomers for these bonds with a marked preference for *trans*. Integration of the areas under the maxima gives the fractions for the two isomers of $p_t \approx 0.728$, $p_c \approx 0.272$ for the lattice and $p_t \approx 0.612$, $p_c \approx 0.388$ for the isolated molecule, both at 300 K, which suggest energy differences of $E_c \approx 0.59$ and 0.27 kcal/mol, respectively, for the lattice and the isolated molecule.

Figs. 6 and 7 show the distribution of a priori probabilities for the skeletal pairs of bonds P–N–P and N–P–N in the lattice system. These two figures indicate the presence of three preferred conformations, namely tt, tc and ct, with a rather small participation of cc orientations, specially in the case of the N–P–N pair of bonds. The tt area for the P–N–P pair of bonds is split into two maxima which are displaced ca 15–20° from the $\phi_{P-N} = \phi_{N-P} = 180°$ orientation in order to relieve the strong interactions among the Cl atoms attached to contiguous skeletal P atoms (see below the definition of conformational energy E_ω).

The results depicted in Figs. 6 and 7 could be written in a more quantitative fashion by integrating the area under the peaks within a given distance $\Delta\phi$ from the maxima. Taking this distance as $\Delta\phi = 40°$, the probability for the allowed conformations of both pairs of skeletal bonds in the lattice could be represented by means of the following matrices where the rotational isomers are taken in the order *cis* ($\phi = 0$), *trans* ($\phi = 180°$), and the values have been

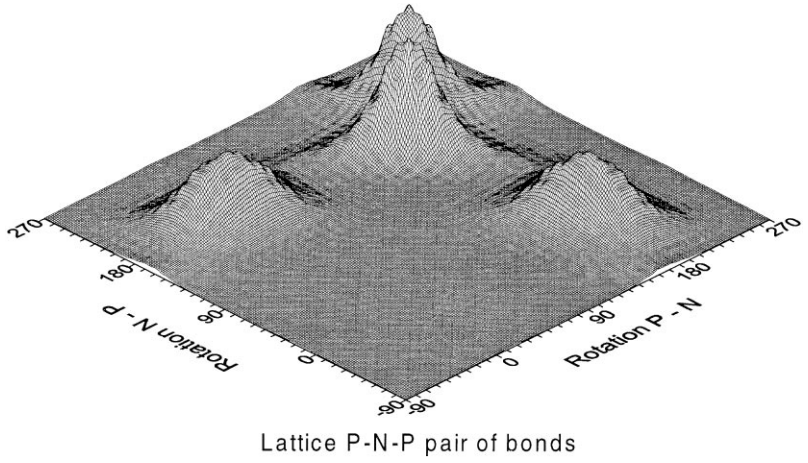

Fig. 6. Distribution of a priori probabilities for the P–N–P pair of skeletal bonds in the lattice. The results were averaged over all alike pairs contained in the fragment of interest.

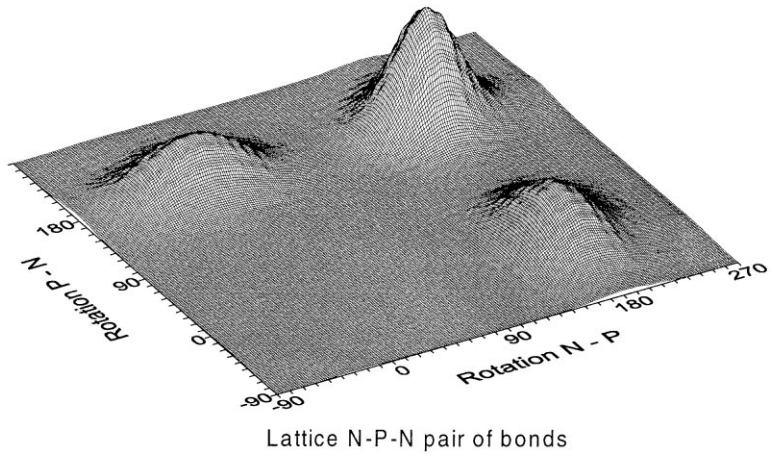

Fig. 7. Distribution of a priori probabilities for the N–P–N pair of skeletal bonds in the lattice (see legend for Fig. 6).

normalized to unity:

$$P_{\mathrm{PNP}} = \begin{bmatrix} 0.0098 & 0.2710 \\ 0.2710 & 0.4482 \end{bmatrix} \quad P_{\mathrm{NPN}} = \begin{bmatrix} 0.0012 & 0.2703 \\ 0.2703 & 0.4582 \end{bmatrix} \tag{6}$$

According to these probabilities, the chain is formed by sequences of two or three bonds in *trans* conformations disrupted by *trans–cis* units while *cis–cis* conformations are quite infrequent, ca 1% in the P–N–P pair of bonds and 0.1% in N–P–N.

The average number of skeletal bonds contained in the all-*trans* sequences can be evaluated with the following scheme. According to Eq. (6), the probability for a P–N bond being in *trans* is $p_t = 0.719$ (i.e. sum of the probabilities for tc and tt in the second row of the P_{PNP} matrix) while the probability for the P–N–P pair of bonds being in tt is $p_{tt} = 0.448$. Thus, the probability of replication (i.e. the probability of a *trans* bond being followed by another *trans*) is $p_r = p_{tt}/p_t = 0.623$, while the probability of inversion (i.e. *trans* bond followed by *cis*) would be $(1 - p_r)$. A sequence of n_t bonds in the all-*trans* conformation requires $n - 1$ replications and one inversion, and therefore, will have a probability of $(p_r)^{n-1}(1 - p_r)$. The average value $\langle n_t \rangle$ can then be evaluated through addition over all the values of n_t as:

$$\langle n_t \rangle = (1 - p_r) \sum_{i=1}^{\infty} i(p_r)^{i-1} = \frac{1}{1 - p_r} \tag{7}$$

which in this case amounts to 2.7 bonds.

The distribution of probabilities for the isolated molecules is represented in Figs. 8 and 9 whose integration, with the same criteria than in the previous case, gives the following results:

$$P_{\mathrm{PNP}} = \begin{bmatrix} 0.1262 & 0.2534 \\ 0.2534 & 0.3670 \end{bmatrix} \quad P_{\mathrm{NPN}} = \begin{bmatrix} 0.0058 & 0.3713 \\ 0.3713 & 0.2516 \end{bmatrix} \tag{8}$$

which indicate a smaller preference for the tt conformations than in the case of the lattice, and therefore, represent a much more compact polymer chain than in the previous

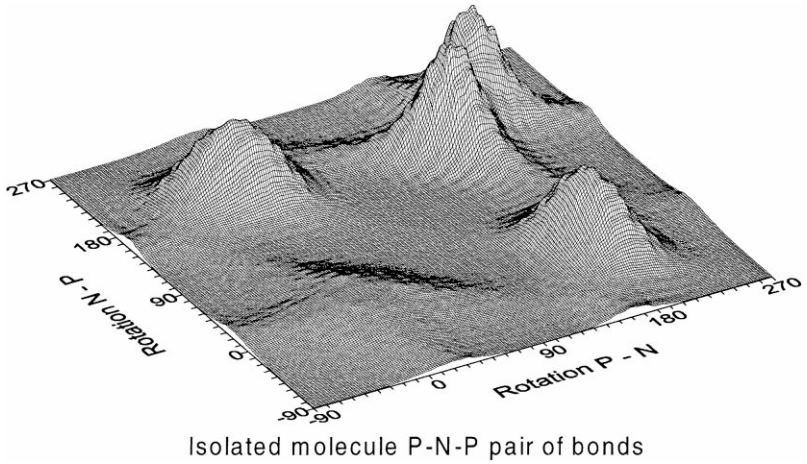

Fig. 8. Distribution of a priori probabilities for the P–N–P pair of skeletal bonds in the isolated molecule (see legend for Fig. 6).

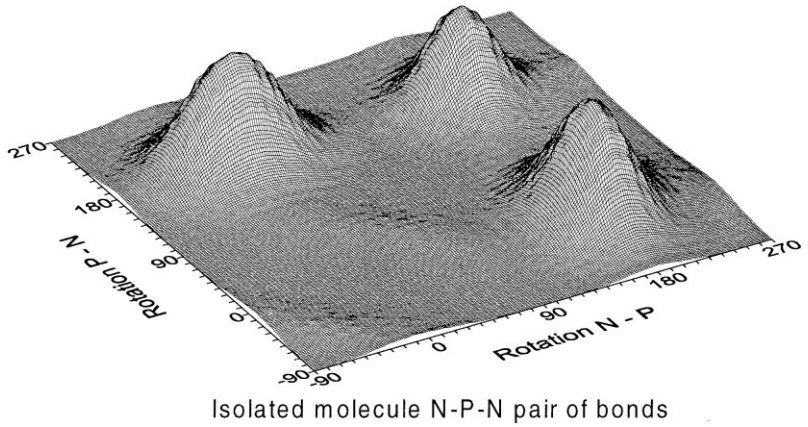

Fig. 9. Distribution of a priori probabilities for the N–P–N pair of skeletal bonds in the isolated molecule (see legend for Fig. 6).

case. For instance, the evaluation of the averaged number of bonds in the all *trans* sequences, taking into account that the probabilities of replication are $p_t = 0.592$ and 0.326, respectively, for PNP and NPN pairs of bonds, amounts to ca $\langle n_t \rangle \approx 1.7$ in this case.

4. Conformational model

It is rather easy to set up a conformational model, based on the rotational isomeric states scheme [19–21], that could be able of reproducing the main features observed in the MD simulation. Thus, taking the rotational isomers in the order *cis* ($\phi_c = 0$) and *trans* ($\phi_t = 180$), the statistical weight matrices for the two different pairs of bonds of the polymer backbone, which are represented in Fig. 10, may be written as:

$$U_{PNP} = \begin{bmatrix} \omega_2 & \omega_1^2 \\ \omega_1^2 & \omega^2 \end{bmatrix} \qquad U_{NPN} = \begin{bmatrix} \omega_4 & \omega_3 \\ \omega_3 & 1 \end{bmatrix} \tag{9}$$

where the *trans–trans* state for the pair of bonds N–P–N has been taken as reference, and the statistical weights ω, ω_1, ω_2, ω_3 and ω_4 are Boltzmann exponentials of their respective energies whose meaning is summarized in Table 2.

The partition function for a chain containing x repeating units may be evaluated by a serial product of these statistical weight matrices as [19,20]:

$$Z = [1\ 0][U_{PNP}U_{NPN}]^{x-1}\begin{bmatrix} 1 \\ 1 \end{bmatrix} \tag{10}$$

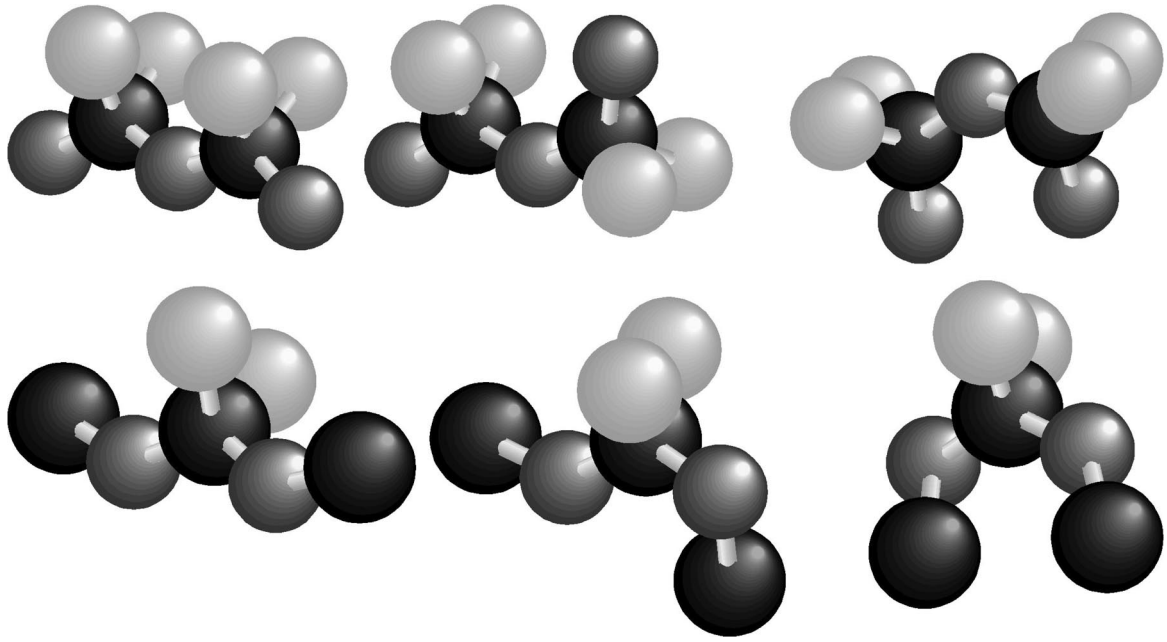

Fig. 10. Representation of the tt, tc and cc conformations for the P–N–P and N–P–N skeletal pairs of bonds illustrating the Cl···Cl; N···Cl; N···N; N···P and P···P second-order interactions that produce, respectively, the conformational energies E_ω, $E_{\omega 1}$, $E_{\omega 2}$, $E_{\omega 3}$ and $E_{\omega 4}$.

Table 2
Statistical weights, normalized to *trans–trans* states, for the U_{PNP} and U_{NPN} matrices representing the conformational states allowed to the P–N–P and N–P–N pairs of skeletal bonds in PDCPN

Statistical weight	Energy	Conformation	Interaction	Order
ω	E_ω	tt in P–N–P	Cl···Cl	Second
ω_1	$E_{\omega 1}$	ct or tc in P–N–P	N···Cl	Second
ω_2	$E_{\omega 2}$	tt in P–N–P	N···N	Second
ω_3	$E_{\omega 3}$	ct or tc in N–P–N	N···P	Second
ω_4	$E_{\omega 4}$	tt in N–P–N	P···P	Second

The a priori probability for a pair of P–N–P bonds within a long chain (for instance, in the center of a chain containing $2x + 2$ repeating units), being in conformational state *ij* (with *i* and *j* representing *cis* or *trans*), may be computed as [19,20]:

$$p_{ij}(\mathrm{PNP}) = Z^{-1}[10][U_{\mathrm{PNP}}U_{\mathrm{NPN}}]^x U^0_{\mathrm{PNP}}U_{\mathrm{NPN}}[U_{\mathrm{PNP}}U_{\mathrm{NPN}}]^x \times \begin{bmatrix} 1 \\ 1 \end{bmatrix} \tag{11}$$

where the U^0_{PNP} matrix is obtained from U_{PNP} by replacing all its elements by zero, except element *ij* which is left unchanged. The same procedure can be used to compute the probabilities for the allowed conformations of the NPN pair of bonds with $U_{PNP}U^0_{PNP}$ in the central part of the equation.

The probabilities for all the allowed conformations of both pairs of bonds can be computed with different values of the conformational energies seeking for the best agreement with the results of these probabilities obtained from MD simulations. Thus, the set of energies: $E_\omega = -0.02$, $E_{\omega 1} = -0.03$, $E_{\omega 2} = 1.57$, $E_{\omega 3} = 0.06$ and $E_{\omega 4} = 3.08$ kcal/mol gives:

$$P_{\mathrm{PNP}} = \begin{bmatrix} 0.010 & 0.266 \\ 0.266 & 0.458 \end{bmatrix} \quad P_{\mathrm{NPN}} = \begin{bmatrix} 0.001 & 0.275 \\ 0.275 & 0.449 \end{bmatrix} \tag{12}$$

in excellent agreement with the results of MD simulations for the lattice summarized in Eq. (6), while the set of values $E_\omega = 0.15$, $E_{\omega 1} = 0.38$, $E_{\omega 2} = 1.41$, $E_{\omega 3} = -0.77$ and $E_{\omega 4} = 1.18$ kcal/mol gives:

$$P_{\mathrm{PNP}} = \begin{bmatrix} 0.126 & 0.253 \\ 0.253 & 0.368 \end{bmatrix} P_{\mathrm{NPN}} = \begin{bmatrix} 0.006 & 0.373 \\ 0.373 & 0.248 \end{bmatrix} \tag{13}$$

in good agreement with the results for the isolated molecule represented by Eq. (8).

Standard procedures of the matrix multiplication scheme [19–21] were employed to generate chains containing different number of repeating units *x*, up to $x = 200$, with the statistical weight matrices represented by Eq. (9). The unperturbed value of the mean squared end to end distance $\langle r^2\rangle_0$ was computed and transformed into the dimensionless characteristic ratio which for $N = 2x = 400$ skeletal bonds has already reached the asymptotic value for very long chains C_∞. The results were $C_\infty = 15.7$ and 8.0, respectively, for the sets of conformational energies representing the lattice and the isolated molecule.

Very few experimental values of the unperturbed dimensions of PDCPN that could be compared with our theoretical results have been reported in the literature [4,15,31,32]. And, what is even worse, those experimental values are quite contradictory since they cover the range from $C_\infty \approx 3$ to 100. Experimental difficulties due to crosslinking of the samples, formation on aggregates or inaccuracy in the extrapolation of results obtained in good solvents to unperturbed conditions have been invoked as reasons for these discrepancies [15]. However, the most reliable results, obtained very close to θ conditions, suggest a value $C_\infty \approx 20$. Under these circumstances, the only assertion that we can make is that the results obtained with the lattice are not bad, and certainly much better than those obtained for the isolated molecule.

It is important to realize that the two rotational states model indicated in Eq. (9) is intended to provide a reasonable description of the average behavior of the chain, but it does not give good pictures of any individual conformation. For instance, since only $\phi = 0$ (*cis*) and $\phi = 180$ (*trans*) orientations are allowed to the backbone rotational angles, any individual conformation generated with this model will be planar, and therefore, very different from actual conformations such as those shown in Figs. 2 and 3. This restriction may be easily removed by splitting the allowed rotational isomers as the probability plots shown in Figs. 6 and 8 suggest. Thus, splitting the *trans* states into $t_-(\phi \approx 160°)$, $t_0 = (\phi = 180°)$ and $t_+(\phi \approx 200°)$, i.e. a displacement of ca. 20° with deviations of the same sign in both rotational angles for the PNP pairs of bonds according to the results shown in Figs. 6 and 8, the statistical weight matrices, with the states in the order *c*, t_-, t_0, t_+, may be written as:

$$U_{\mathrm{PNP}} = \begin{bmatrix} \omega_2 & 0 & \omega_1^2 & 0 \\ 0 & \omega^2/2 & 0 & 0 \\ \omega_1^2 & 0 & 0 & 0 \\ 0 & 0 & 0 & \omega^2/2 \end{bmatrix}$$
$$U_{\mathrm{NPN}} = \begin{bmatrix} \omega_4 & \omega_3 & \omega_3 & \omega_3 \\ \omega_3 & 1 & 1 & 1 \\ \omega_3 & 1 & 1 & 1 \\ \omega_3 & 1 & 1 & 1 \end{bmatrix} \tag{14}$$

This four states model produces three-dimensional (3D) conformations similar to the actual ones adopted by the chain and, of course, gives a better description of the average behavior than the two states model. However, calculation of averaged molecular dimensions performed with this model proved that the values of C_∞ calculated with the two

and four states schemes differ only in ca. 10% and for that reason, we prefer to use the easier two states model in this paper.

On the other hand, although the statistical weights ωs may be related to short range interactions (see Table 2 and Fig. 10), they are not calculated by computing those interactions. On the contrary, a very large number of actual conformations adopted by a relatively long segment (i.e. 18 repeat units) embedded within a much longer oligomer (i.e. 56 repeat units) were analyzed seeking for the probability of incidence of every allowed orientation, which will depend on all interactions occurring in the system, including both short- and long-range interactions as well as intermolecular interactions in the case of the lattice. This is the reason why, even if the short-range interactions are identical for the lattice and the isolated molecule, the probability matrices for these systems, represented, respectively, by Eqs. (6) and (8), are quite different, reflecting the fact that extended conformations are more frequently adopted in the lattice than in the case of the isolated molecule.

5. Discussion

The fact that the lattice and the isolated molecule behave on very different ways has appeared many times above, e.g. compare solid and dot lines in Fig. 5, probability distributions of Figs. 6 and 7 and Eq. (6) with those in Figs. 8 and 9 and Eq. (8), values of $\langle n_t \rangle$ and C_∞ for the two systems, etc. All these results indicate that the lattice has a larger preference for *trans*, and therefore, produce more extended conformations, than the isolated molecule. However, this difference may be observed in a much more visual approach by comparing Figs. 2 and 3. Certainly these figures represent only one among the almost infinite number of conformations allowed to these systems, or even among the 5×10^4 conformations analyzed for the whole MD simulation, but examination of the results indicates that conformations similar to those represented in Figs. 2 and 3 are frequently visited by these systems.

And now, the important question is, why these two systems, which after all represent the same oligomer, behave in such different ways? The main difference among these two systems lies in the way of dealing with long-range intramolecular interactions, i.e. interactions among atoms separated by more than two skeletal bonds. In the case of the lattice, these interactions are compensated by intermolecular interactions between the primary chain and its images lying within the box, while there is no compensation of any kind in the case of the isolated molecule that may fold over itself in order to place different segments in relative orientations that would produce neat long range attractions and consequently, the more compact conformations are then favored. Long-range interactions are produced both by Coulombic and van der Waals forces. In the case of PDCPN, and probably in many other PPNs, the partial charges on the skeletal atoms are rather high according to quantum mechanics calculations [6,11,16], which suggests that Coulombic forces may be strong. But, on the other hand, the ϵ parameter governing the strength of the van der Waals interactions (see Eq. (4) and Table 1) is larger for Cl, N and P atoms than for C and H, and consequently, when these atoms are placed at the appropriate distance, rather strong attractions may be raised which will be much stronger than in the case of hydrocarbon chains such as polystyrene, for instance.

Some exploratory calculations were performed in order to ascertain the effect of Coulombic interactions on the general features of the polymer. The results of these calculations are most surprising. First of all, when a distance-independent dielectric constant is employed, i.e. taking $\epsilon(r_{ij}) = \epsilon_0 =$ constant in Eq. (5), the results obtained are virtually identical to those computed with Eq. (5) which are shown in Figs. 8 and 9 and Eq. (8). The reason is that all the significant interactions are produced when the distance among the interacting atoms lies within a rather narrow interval, ca. $3.1 - 4.2$ Å, as it can be seen by calculating the distances among the interacting atoms on the conformations represented in Fig. 10 that define first and second-order interactions for the allowed conformations of the chain. However, removal of Coulombic interactions produces a noticeable increase of *cis* conformations, both in the isolated molecule and the lattice system. For instance, the probability matrices for the isolated molecule, equivalent to Eq. (8) when electrostatic interactions are taken into account, become in this case:

$$P_{PNP} = \begin{bmatrix} 0.2056 & 0.2566 \\ 0.2566 & 0.2812 \end{bmatrix} \quad P_{NPN} = \begin{bmatrix} 0.0160 & 0.4203 \\ 0.4203 & 0.1434 \end{bmatrix} \tag{15}$$

Thus, removal of Coulombic interactions produces a substantial increase of cc conformations with a consequent decrease of tt states for the PNP pair of bonds which reach an almost freely rotating situation. This effect is much smaller in the case of the NPN pair of bonds although it also goes in the sense of decreasing the probability of the most extended conformation. Molecular dimensions are therefore decreased and $C_\infty = 6.1$ is obtained with the probabilities shown in Eq. (15).

It is easy to rationalize the variation of probabilities produced by removal of electrostatics. Thus, in the case of PNP pair of bonds, the interactions produced in the four allowed states are: E_ω in tt due to the Cl···Cl interaction whose Coulombic contribution depends on the partial charge over Cl atoms, i.e. $E_{coul} \sim (q_{Cl})^2 = (-0.451)^2$; $E_{\omega 1}$ in tc arising from N···Cl interactions in which $E_{coul} \sim (q_N q_{Cl}) = (-0.451)(-0.919)$ $E_{\omega 2}$ in cc from N···N with $E_{coul} \sim (q_N)^2 = (-0.919)^2$. Coulombic interactions are repulsive in the three cases, but their strength increases from tt to cc and therefore the tt state is disfavored by removal of these interactions. In the case of

the NPN pair of bonds, Coulombic interactions are repulsive for the cc state and attractive for the other two, and for this reason cc is favored by removal of these interactions, although it still keeps a very low probability due to van der Waals interactions. Coulombic interactions are attractive and almost identical in ct and tt states of the NPN pair of bonds, so that their relative probabilities does not change substantially when these interactions are removed. The reason is that they are mainly due to the two Cl···P pairs (first-order interaction) and the N···P (second-order interaction); the distance, in Å, among these atoms are $r_{ClP} \approx 3.5$, $r_{NP} \approx 4.3$ in tt and $r_{ClP} \approx 4.2$, $r_{NP} \approx 3.3$ for tc.

The effect of electrostatic interactions on the lattice system is similar to that produced on the isolated molecule. Thus, removal of these interactions provides the following probabilities for the lattice:

$$P_{PNP} = \begin{bmatrix} 0.0745 & 0.3454 \\ 0.3454 & 0.2347 \end{bmatrix} \quad P_{NPN} = \begin{bmatrix} 0.0056 & 0.3932 \\ 0.3932 & 0.2080 \end{bmatrix} \tag{16}$$

Comparison of these values with those indicated in Eq. (6), where the Coulombic interactions were taken into account, shows a substantial increase of tc and ct conformations at the expense of tt. Calculation of the molecular dimensions for this system provides $C_\infty = 12.5$ which is noticeably smaller than the value 15.7 obtained when the Coulombic interactions are considered, but still much higher than the results found for the isolated molecule.

However, this artificial removal of electrostatic interactions probably is not a realistic simulation of the effect produced in the system by a change on the polarity of the solvent or even by the addition of ionic salts. Thus, *all electrostatic interactions* are removed in the calculation regardless of the distance among the interacting atoms, while the effect of the solvent will be to solvate the chain and modify the interactions among atoms that are separated by a distance large enough as to allow a molecule of solvent to be placed in between. Consequently, short-range interactions among atoms separated by ca. 3–4 Å should be scarcely affected by the solvent. On the contrary, since the chain holds large atomic partial charges, polar solvents may produce a better solvation, thus favoring the extended conformations as in the case of the lattice.

Thus, it seems that long-range interactions, mostly due to van der Waals forces, play an important role on the probability distribution of the conformations allowed to this polymer, and therefore, produce a dramatic change on the averaged value of its molecular dimensions. If this interpretation was correct, it would also show up in the experimental results obtained from measurements performed in solution. A rather strong effect of the solvent in the values of $\langle r^2 \rangle$, from solvents that will not compensate the intramolecular interactions, thus producing low values of $\langle r^2 \rangle$ to situations in which the solvent–polymer interactions may be very strong and consequently will give very high dimensions. On the other hand, this prominent role of the solvent will increase the difficulty and decrease the accuracy of any extrapolation procedure employed for obtaining unperturbed dimensions. This is exactly the situation described in many experimental studies of PPNs: wildly different results and inaccurate extrapolations. A good example is provided by the experimental determinations of the molecular dimensions of PDCPN from viscometric measurements in toluene (low polarity solvent) and chloroform (high polarity) solutions that gave [15,31] $C'_\infty \approx 3.3$ and 20, respectively (where $C'_\infty = \langle r^2 \rangle / Nl^2$ represents the characteristic ratio obtained with perturbed values $\langle r^2 \rangle$ instead of unperturbed $\langle r^2 \rangle_0$ as C_∞).

Furthermore, a well-known *experimental trick* when working on size exclusion chromatography of PPNs employing low polarity eluents consists in the addition of small amounts of quaternary ammonium salts in order to eliminate *anomalous* signals at high elution volumes [33–35], i.e. low molecular dimensions. These signals may be produced by chains collapsed to highly compact conformations by the effect of intramolecular interactions that will become less intense when some ions are added to the solution, thus favoring the solvation of the chain. Finally, some experimental determinations of radius of gyration of several PPNs, mainly obtained by light scattering of solutions in low polarity solvents, report a scaling law $\langle S^2 \rangle^{1/2} = \mathrm{QM}^q$ with values of ca $q \approx 1/3$ for the exponent [4,35,36], which suggest polymer chains having a globular shape very similar to most of the conformations adopted by the isolated chain along the MD simulation, for instance, the one represented in Fig. 3. These same studies show *anomalous* up turns of the $\log(\langle s^2 \rangle^{1/2})$ versus $\log(M)$ plots in the region of low molecular masses, suggesting that the size of the chain *decreases with increasing M*. These up turns could also be explained on the grounds of long-range interactions because the chain requires a minimum length before a u-turn may be produced without raising very strong van der Waals repulsions. Our simulations on PDCPN show that this minimum length is about 10 repeating units in this polymer, but it may be substantially increased in other PPNs bearing bulky side groups.

Of course, we are aware that the solutions of PPNs are rather complicated systems and probably it will require much more time and effort to understand their behavior. But, we would like to stress the point that long-range intramolecular interactions may play an important role in the *peculiarities* of these systems.

Acknowledgements

This work was supported by the DGICYT through grant number PB97-0778. The assistance provided by Dr. D.O. Castaño, who performed the ab initio calculations of the atomic partial charges, is gratefully acknowledged.

References

[1] Potin Ph, De Jaeger R. Eur Polym J 1991;27:341.
[2] Mark JE, Allcock HR, West R. Inorganic polymers. Englewood Cliffs, NJ: Prentice-Hall, 1992 chap. 3.
[3] Manners I. Angew Chem Int Ed Engl 1996;35:1602.
[4] Tarazona MP. Polymer 1994;35:819.
[5] Tarazona MP, Saiz E. In: Salamone JC, editor. Polymeric materials encyclopedia, vol. 9. Boca Raton, FL: CRC Press, 1994. p. 6563.
[6] Tanaka K, Yamashita S, Yamabe T. Macromolecules 1986;19:2062.
[7] Ferris KF, Risser SM. Chem Phys Lett 1990;174:333.
[8] Bougeard D, Bremard C, Jaeger RD, Lemmouchi Y. J Phys Chem 1992;96:8850.
[9] Boehm RC. J Phys Chem 1993;97:13877.
[10] Amato ME, Lipkowitz KB, Lombardo GM, Pappalardo GC. J Mol Struc 1995;372:69.
[11] Sun H. J Am Chem Soc 1997;119:3611.
[12] Allcock HR, Allen RW, Meister JJ. Macromolecules 1976;9:950.
[13] Allen RW, Allcock HR. Macromolecules 1976;9:956.
[14] Boyd RH, Kesner L. J Am Chem Soc 1977;99:4248.
[15] Saiz E. J Polym Sci B, Polym Phys Ed 1987;25:1565.
[16] Caminiti R, Gleria M, Lipkowitz KB, Lombardo GM, Pappalardo GC. J Am Chem Soc 1997;119:2204.
[17] Tarazona MP, Bravo J, Rodrigo MM, Saiz E. Polym Bull 1991;26:465.
[18] Ramos-Vieira A, Tarazona MP, Saiz E. Polymer 1997;38:1919.
[19] Flory PJ. Statistical mechanics of chain molecules. New York: Interscience, 1969.
[20] Flory PJ. Macromolecules 1974;7:381.
[21] Riande E, Saiz E. Dipole moments and birefringence of polymers. Englewood Cliffs, NJ: Prentice-Hall, 1992.
[22] Forester TR, Smith W. DL_POLY (Ver. 2.10), Daresbury Laboratory, Daresbury, Warrington WA4 4AD, UK.
[23] Allen MP, Tildesley DJ. Computer simulation of liquids. Oxford: Clarendon, 1987.
[24] Riande E, Saiz E. Curr Trends Polym Sci 1997;2:1.
[25] Brooks BR, Bruccoleri RE, Olafson BD, States DJ, Swaminathan S, Karplus M. J Comp Chem 1983;4:187.
[26] Weiner SJ, Kollman PA, Case DA, Singh UC, Ghio C, Alagona G, Profeta Jr S, Weiner P. J Am Chem Soc 1984;106:765.
[27] Weiner SJ, Kollman PA, Nguyen DT, Case DA. J Comp Chem 1986;7:230.
[28] Homans SW. Biochemistry 1990;29:9110.
[29] Cornell WD, Cieplak P, Bayly CL, Gould IR, Merz KM, Ferguson DM, Spellmeyer DC, Fox T, Caldwell JW, Kollman PA. J Am Chem Soc 1995;117:5179.
[30] Frisch MJ, Trucks GW, Schlegel HB, Gill PMW, Johnson BG, Robb MA, Cheeseman JR, Keith T, Petersson GA, Montgomery JA, Raghavachari K, AlLaham MA, Zakrzewski VG, Ortiz JV, Foresman JB, Cioslowski J, Stefanov BB, Nanayakkara A, Challacombe M, Peng CY, Ayala PY, Chen W, Wong MW, Andres JL, Replogle ES, Gomperts R, Martin RL, Fox DJ, Binkley JS, Defrees DJ, Baker J, Stewart JP, HeadGordon M, Gonzalez C, Pople JA. GAUSSIAN94, Revision E.2, Gaussian, Inc., Pittsburgh, PA, 1995.
[31] Patat F, Kollinsky F. Makromol Chem 1951;6:292.
[32] Knoesel K, Parrod J, Benoit H. Comp Rend 1960;251:2944.
[33] Neilson RH, Hani R, Wisian-Neilson P, Meister JS, Roy AK, Hagnauer GL. Macromolecules 1987;20:910.
[34] Bravo J, Tarazona MP, Saiz E. Macromolecules 1991;24:4089.
[35] Bravo J, Tarazona MP, Saiz E. Macromolecules 1992;25:5625.
[36] Búrdalo J, Tarazona MP, Carriedo G, Garcia-Alonso FJ, González P. Polymer 1999;40:4251.